JOC The Journal of Organic Chemistry

Article

pubs.acs.org/joc

# Electrophilic Assistance to the Cleavage of an RNA Model Phopshodiester via Specific and General Base-Catalyzed Mechanisms

David Octavio Corona-Martínez,[†] Paola Gomez-Tagle,[‡] and Anatoly K. Yatsimirsky*[,‡]

[†]Universidad de Sonora, Campus Cajeme, División de Ciencias Biológicas y de la Salud, 85000 Ciudad Obregón, Sonora, México

[‡]Facultad de Química, Universidad Nacional Autónoma de México, 04510 México D.F., México

Supporting Information

**ABSTRACT:** Kinetics of transesterification of the RNA model substrate 2-hydroxypropyl 4-nitrophenyl phosphate promoted by $Mg^{2+}$ and $Ca^{2+}$, the most common biological metals acting as cofactors for nuclease enzymes and ribozymes, as well as by $Co(NH_3)_6^{3+}$, $Co(en)_3^{3+}$, $Li^+$, and $Na^+$ cations, often employed as mechanistic probes, was studied in 80% v/v (50 mol %) aqueous DMSO, a medium that allows one to discriminate easily specific base ($OH^-$-catalyzed) and general base (buffer-catalyzed) reaction paths. All cations assist the specific base reaction, but only $Mg^{2+}$ and $Na^+$ assist the general base reaction. For $Mg^{2+}$-assisted reactions, the solvent deuterium isotope effects are 1.23 and 0.25 for general base and specific base mechanisms, respectively. Rate constants for $Mg^{2+}$-assisted general base reactions measured with different bases fit the Brønsted correlation with a slope of 0.38, significantly lower than the slope for the unassisted general base reaction (0.77). Transition state binding constants for catalysts in the specific base reaction ($K^{\ddagger}_{OH}$) both in aqueous DMSO and pure water correlate with their binding constants to 4-nitrophenyl phosphate dianion ($K_{NPP}$) used as a minimalist transition state model. It was found that $K^{\ddagger}_{OH} \approx K_{NPP}$ for "protic" catalysts ($Co(NH_3)_6^{3+}$, $Co(en)_3^{3+}$, guanidinium), but $K^{\ddagger}_{OH} \gg K_{NPP}$ for $Mg^{2+}$ and $Ca^{2+}$ acting as Lewis acids. It appears from results of this study that $Mg^{2+}$ is unique in its ability to assist efficiently the general base-catalyzed transesterification often occurring in active sites of nuclease enzymes and ribozymes.

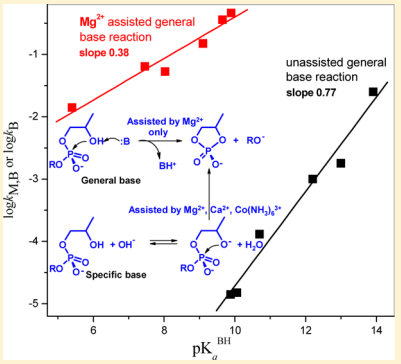


## INTRODUCTION

Rapidly growing information on detailed mechanisms of action of nuclease enzymes and ribozymes reveals a large diversity of possible roles played by metal ions and acid−base functional groups in the transition state stabilization.[1] An essential part of all proposed mechanisms is the electrophilic assistance to the nucleophilic attack on the phosphoryl group provided either by a Lewis acid (typically $Mg^{2+}$, $Ca^{2+}$, or $Zn^{2+}$) or by a protic acid (imidazolium, ammonium, or guanidinium groups). The latter can operate as a general acid catalyst by proton transfer or provide the electrostatic stabilization for the anionic transition state.

In most cases the RNA cleavage occurs by the action of 2′-OH ribose functionality as an internal nucleophile. In biological systems the nucleophilic attack is assisted by general base catalysis, but chemical transesterification/hydrolysis of phosphodiesters possessing a $\beta$-hydroxyl group proceeds mostly through equilibrium predissociation of hydroxyl group with subsequent nucleophilic attack of the alkoxide on the phosphodiester group (Scheme 1),[2,3] which can be formally considered as a specific base mechanism. It has been shown that metal complex catalysis in such reactions involves an electrophilic assistance to the last step by the aquo form of the complex (M in Scheme 1), whereas the hydroxo form of the complex is inactive.[4]

A slow general base-catalyzed path does exist but can be detected in the background of much faster specific base reaction

**Scheme 1**

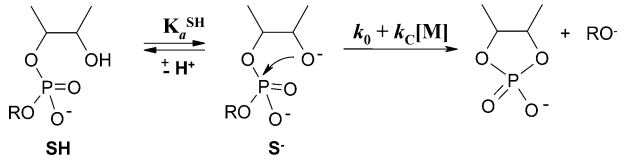


only at very high concentrations of bases, which significantly affect the reaction medium and make rather ambiguous the interpretation of kinetic results.[1c,5] In particular, enzyme-like mechanisms involving electrophilic assistance to general base mechanism of transesterification by a protonated base or by a metal ion reported in earlier studies were not confirmed later and appeared to be artifacts of medium effects[6] or metal complexation by a base as a ligand,[7] respectively. Recently, it has been shown that changing the reaction medium from water to 80% v/v (50 mol %) aqueous DMSO leads to a strong suppression of the specific base hydrolysis at a given pH, allowing direct observation of the general base reaction path at much lower base concentrations and free of possible complications.[8] Under these conditions it was possible to observe for the first time a clear "bell-shaped" second-order in catalyst kinetics of buffer catalysis reminiscent of the classical

**Received:** August 3, 2012
**Published:** September 19, 2012

   dx.doi.org/10.1021/jo301649u | J. Org. Chem. 2012, 77, 9110−9119

**Scheme 2**

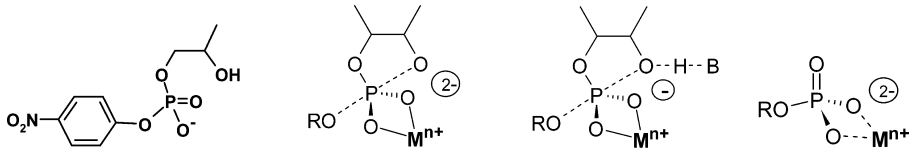


mechanism of RNA-se A. In this paper we apply a similar approach to analyze the Lewis acid assistance to the general base catalysis by some of the most common cations acting as cofactors for nuclease enzymes and ribozymes, namely, $Mg^{2+}$ and $Ca^{2+}$. Also the effect of alkali cations ($Na^+$, $Li^+$) was studied for comparison.

A particular case of electrophilic assistance is the outer-sphere mechanism proposed for some Mg(II)-dependent enzymes and ribozymes where the aqua-ion $Mg(H_2O)_6^{2+}$ provides the transition state stabilization by hydrogen bonding to protons of coordinated water molecules.[1b,d,9] Chemical catalysis in phosphodiester cleavage by protic acids is generally much less efficient than that achieved by Lewis acids, and for this reason it seems surprising that a kinetically labile metal ion may act via an outer-sphere rather than an inner-sphere mechanism. The most common experimental test for the outer-sphere mechanism is the retention of catalytic activity when Mg(II) is substituted with a kinetically inert complex such as $Co(NH_3)_6^{3+}$.[9,10] Surprisingly, the efficiency of catalysis by Co(III) ammine complexes was never compared with that of Mg(II) in model systems, and for this reason we included in this study also an investigation of catalysis by $Co(NH_3)_6^{3+}$ and $Co(en)_3^{3+}$ complexes.

A simple RNA-type model substrate 2-hydroxypropyl 4-nitophenyl phosphate (HPNP) was employed, which allows one a convenient spectrophotometric monitoring of the rate of intramolecular transesterification. Low basicity of the 4-nitrophenolate makes unlikely any kind of electrophilic leaving group assistance either by a protic or a Lewis acid. Therefore the most probable mechanism of catalysis with HPNP as a substrate is binding of metal ion or a proton donor to equatorial oxygens in the phosphorane transition state as illustrated in Scheme 2 for cooperation of the metal ion with specific base (**1**) or general base (**2**) reactions (encircled negative charges refer to phosphate parts of the transition states and are not the total charges).

Studies in a mixed aqueous DMSO solvent were complemented with studies in pure water where only the specific base reaction was observed. In conclusion we analyze correlations between transition state stabilization free energy and binding free energy of the catalysts to a $ROPO_3^{2-}$ dianion considered as a crude transition state model for the specific base reaction (**3** in Scheme 2).

## RESULTS AND DISCUSSION

**Catalysis in 80% v/v Aqueous DMSO.** The majority of kinetic measurements were performed in 0.1 M piperidine/HCl buffer solutions containing from 10% to 70% free base. This corresponds to variation in pH from 8.9 to 10.3. With p$K_w$ of 18.77 in this medium these are essentially neutral solutions with very low concentration of free hydroxide ions from $1.2 \times 10^{-10}$ to $3.2 \times 10^{-9}$ M. The rate constants of specific base and general base-catalyzed reactions in this medium are $k_{OH} = 0.58\ M^{-1}\ s^{-1}$ and $k_B = 1.4 \times 10^{-5}\ M^{-1}\ s^{-1}$.[8] Therefore the maximum contribution of the specific base catalysis to the observed rate constant of transesterification in the absence of metal ion is $k_{OH}[OH^-] = 1.9 \times 10^{-9}\ s^{-1}$. The corresponding contribution of the general base catalysis is $k_B[B] = 1 \times 10^{-6}\ s^{-1}$, and obviously this is the principal reaction path in the absence of metal ions. However, the dianionic transition state of the specific base reaction can be stabilized much more efficiently than the monoanionic transition state of the general base reaction by the electrophilic assistance, and this can make the contribution of the specific base reaction significant in the presence of metal ions or other electrophilic catalysts.

A general expression for the observed first-order rate constant of HPNP transesterification has the form

$$k_{obs} = k_{OH}[OH^-] + k_B[B] + k_{B,BH}[B][BH] + k_{M,OH}[M][OH^-] + k_{M,B}[M][B] \quad (1)$$

The second-order rate constant of the catalytic reaction $k_2$ was calculated as the slope of the plot of $k_{obs}$ versus catalyst concentration [M] at fixed pH, eq 2:

$$k_2 = \frac{dk_{obs}}{d[M]} = k_{M,OH}[OH^-] + k_{M,B}[B] \quad (2)$$

The individual rate constants $k_{M,OH}$ and $k_{M,B}$ that correspond to cooperation of the metal ion or other electrophilic catalyst with specific base or general base catalysis, respectively, were determined from two series of experiments. In the first series, rate constants $k_2$ were measured in buffer solutions of constant total buffer concentration, but variable proportions of protonated (BH) and neutral (B) forms. In this case both the concentration of free base and the concentration of free hydroxide anions are variable since they are related by eq 3:

$$[OH^-] = \left(\frac{K_w}{K_a}\right)\left(\frac{[B]}{[BH]}\right) \quad (3)$$

If only one term in eq 2 is significant, the $k_2$ must be proportional to either [B] or [B]/[BH] with coefficients of proportionality $k_{M,B}$ or $k_{M,OH}$, respectively. If both terms are significant the $k_2$ must be a nonlinear function of either [B] or [B]/[BH], and the respective rate constants can be calculated from eq 2 by multiparameter correlation. In the second series rate constants $k_2$ were measured in a buffer solution of constant [B]/[BH] ratio but variable total buffer concentration. In this case, only the concentration of free base is variable, and the concentration of free hydroxide anions is constant and is determined by eq 3. Equation 2 now allows one to calculate $k_{M,B}$ from the slope of the dependence of $k_2$ on total buffer concentration and $k_{M,OH}$ from the intercept.

Results for $Ca^{2+}$ in 0.1 M piperidine buffer with various degree of neutralization from 10% to 70% free base are shown in Figure 1. As one can see from Figure 1a, the reaction in the


dx.doi.org/10.1021/jo301649u | J. Org. Chem. 2012, 77, 9110−9119

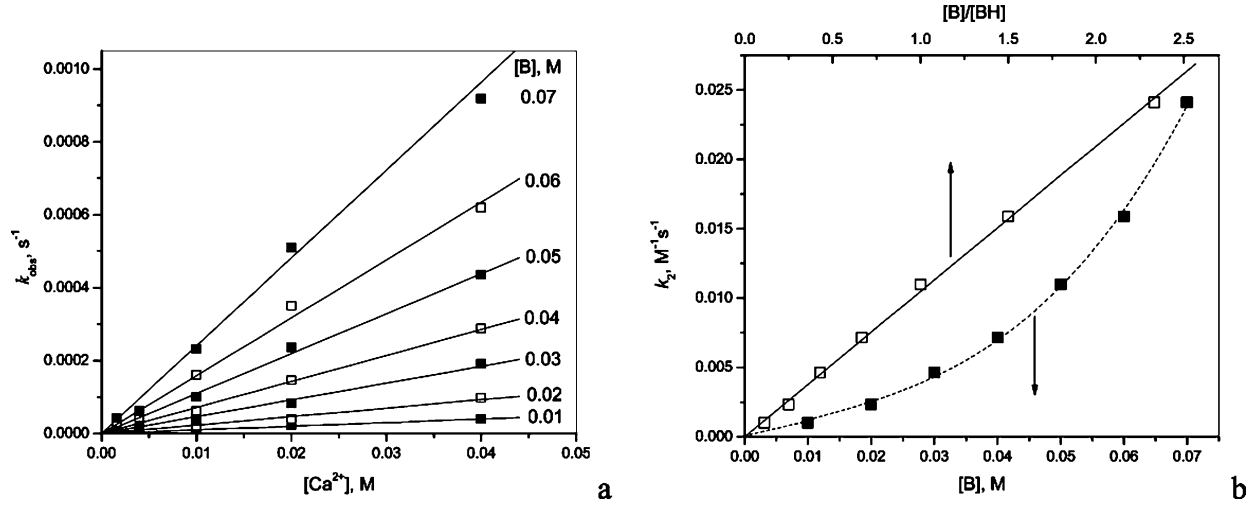


**Figure 1.** Catalysis by $Ca^{2+}$ in 0.1 M piperidine buffer in 80% v/v DMSO. (a) Plots of $k_{obs}$ versus metal ion concentration. (b) Plots of $k_2$ versus concentration of free base [B] (solid squares, lower scale) or versus [B]/[BH] (open squares, upper scale).

**Table 1. Kinetic and Thermodynamic Parameters of HPNP Transesterification in 80% v/v DMSO at 37°C (B = Piperidine)**

| catalyst | $k_{M,B}$ ($M^{-2}$ $s^{-1}$) | $k_{M,OH}$ ($M^{-2}$ $s^{-1}$) | log $K^{\ddagger}_{B}$ | log $K^{\ddagger}_{OH}$ | log $K_{NPP}$ [b] |
|---|---|---|---|---|---|
| $Ca^{2+}$ | | (8.13 ± 0.3) × $10^6$ | 7.14 | 4.63 | |
| $Mg^{2+}$ | 0.46 ± 0.05 | (5.0 ± 0.5) × $10^7$ | 4.5 | 7.9 | 5.22 |
| $Li^+$ | | (2.30 ± 0.06) × $10^4$ | | 4.6 | 2.9[a] |
| $Na^+$ | (1.7 ± 0.2) × $10^{-4}$ | (1.70 ± 0.09) × $10^2$ | 1.1 | 2.5 | 2.2[a] |
| $Co(NH_3)_6^{3+}$ | | (5 ± 1) × $10^5$ | | 5.9 | 5.45 |
| $Co(En)_3^{3+}$ | | (8.4 ± 0.5) × $10^5$ | | 6.2 | |
| $HGu^+$ | 0.0017[8] | | 2.0 | | 2.70 |

[a]In 85% DMSO, from ref 11. [b]Relative error in the range from ±0.05 to ±0.08.

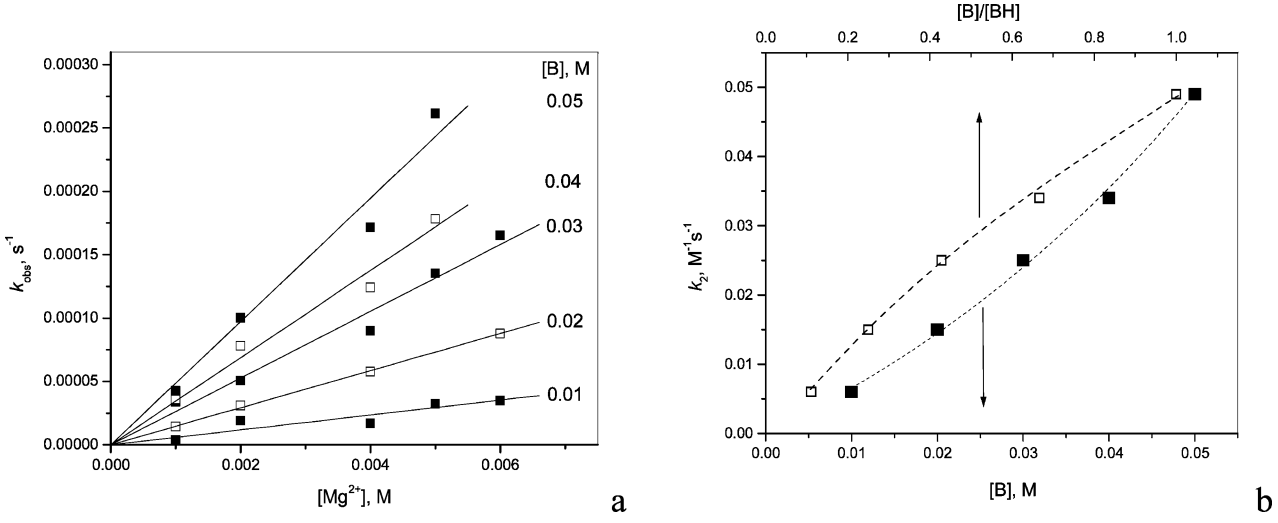


**Figure 2.** Catalysis by $Mg^{2+}$ in 0.1 M piperidine buffer in 80% v/v DMSO. (a) Plots of $k_{obs}$ versus metal ion concentration. (b) Plots of $k_2$ versus concentration of free base [B] (solid squares, lower scale) or versus [B]/[BH] (open squares, upper scale).

presence of Ca(II) is first-order in metal ion, and the acceleration effect over the background reaction is about $10^3$ at 0.04 M Ca(II). The second-order catalytic rate constant is not proportional to the base concentration; however, it is strictly proportional to the [B]/[BH] ratio, that is, to [$OH^-$] (Figure 1b, solid and open squares, respectively). The third-order rate constant $k_{M,OH}$ calculated from the slope of the line in Figure 1b is given in Table 1. The absence of any contribution of the general base-catalyzed reaction assisted by Ca(II) was confirmed by independence of the reaction rate on total buffer concentration at 50% free base fraction in the presence of Ca(II). Thus the electrophilic assistance by Ca(II) leads to the actual acceleration effect of the specific base reaction by a factor of $10^6$, but there is no detectable effect on the general base reaction, which in the absence of metal is a 1000-fold faster than the specific base reaction.

Similar results with Mg(II) are shown in Figure 2. Measurements were performed only up to 50% free base


dx.doi.org/10.1021/jo301649u | J. Org. Chem. 2012, 77, 9110−9119

because of precipitation of $Mg(OH)_2$ in more basic solutions. The overall catalytic activity of Mg(II) is about 5 times larger than that of Ca(II) at the same free base fraction. The reaction is also first-order in metal ion (Figure 2a), but the plot of $k_2$ versus base concentration has a smaller upward curvature, and the plot of $k_2$ versus [B]/[BH] ratio is curved downward (Figure 2b). This means that both terms in eq 2 are significant.

Figure 3 shows the dependences of $k_2$ on total buffer concentration at two degrees of neutralization, which confirms

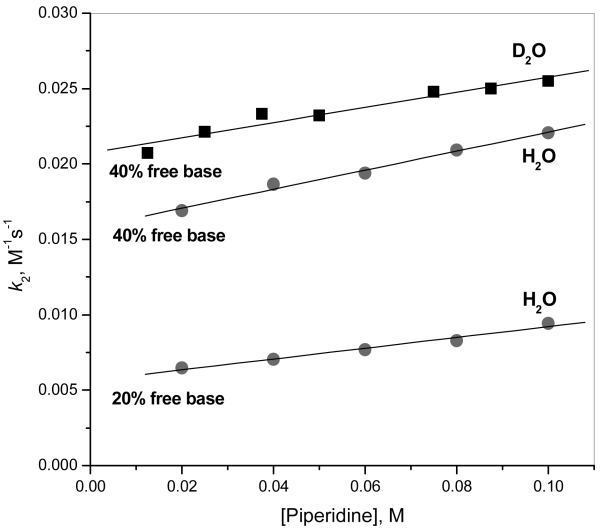


**Figure 3.** Catalysis by $MgCl_2$ in piperidine buffer at variable total buffer concentration in 80% v/v DMSO. Circles show results in DMSO/$H_2O$, and squares show results in DMSO/$D_2O$.

this conclusion: the slopes are nonzero, and both slopes and intercepts of the lines increase on increasing the fraction of free base. The average values of $k_{M,OH}$ and $k_{M,B}$ calculated from both types of experiments are given in Table 1.

Among alkali metal ions only $Li^+$ and $Na^+$ showed noticeable catalytic effects. In case of $Li^+$ only assistance to specific base reaction was observed (see Figure 1S in Supporting Information). Catalysis by $Na^+$ was very weak, but in contrast to other cations sodium did not precipitate in basic solutions, and this allowed us to measure its activity in unbuffered solutions in the presence of a relatively high known concentration of free hydroxide (Figure 2S in Supporting Information) from which $k_{M,OH}$ can be directly calculated. Then, catalysis by $Na^+$ was measured in piperidine buffer (Figure 3S in Supporting Information), and after correction for the contribution of specific base reaction the $k_{M,B}$ was calculated. Both rate constants are given in Table 1.

Measurements with $Co(NH_3)_6^{3+}$ were limited by unexpectedly low solubility of the hydroxide, which precipitated already at pH of about 9.5. Reaction rates measured in piperidine buffer with less than 50% free base were independent of total buffer concentration, and experiments at variable [B]/[BH] ratio indicated the catalytic effect on the specific base reaction only. Similar results were obtained with $Co(en)_3^{3+}$ (Figure 4S in Supporting Information). The respective third-order rate constants are given in Table 1 together with the previously determined catalytic rate constant for guanidinium cation.

Inspection of results collected in Table 1 indicates the following general trends. The catalytic activity in the specific base reaction decreases in the order $Mg^{2+} > Ca^{2+} > Co(NH_3)_6^{3+} \approx Co(en)_3^{3+} > Li^+ \gg Na^+$, which closely follows the order of decreasing charge density ($Z/r_i$) of cations and points principally to electrostatic catalysis. Only $Mg^{2+}$ and $Na^+$ assist the general base reaction. The fact that only $Mg^{2+}$ but not $Ca^{2+}$ can assist the general base reaction is rather surprising. Of course, $Mg^{2+}$ is a stronger electrophile, but by itself that does not mean that it should be relatively more efficient in promoting the general base reaction. Indeed, on going from $Mg^{2+}$ to the much weaker electrophile $Na^+$ the rate constant $k_{M,OH}$ decreases by a factor of $3 \times 10^5$, but $k_{M,B}$ only by a factor of $3 \times 10^3$, which means that for reaction assisted by $Na^+$ the general base path contributes actually more than for $Mg^{2+}$-assisted reaction. Among alkali metal ions, the more electrophilic $Li^+$ catalyzes only specific base reaction, but $Na^+$ shows catalytic activity in both reaction paths. Apparently, there are some requirements most probably related to details of the structure of the coordination sphere and hydration of metal ion that cannot be identified at the moment, needed for efficient electrophilic assistance in general base reaction. Interestingly, guanidinium cation with a smaller charge density than $Na^+$ is a more efficient catalyst for the general base reaction, which may be related to its high efficiency of bidentate binding to phosphate anions.[12]

A useful way to analyze catalytic effects is to see them in terms of transition state stabilization of the unassisted reaction.[13,14] The respective transition state "binding constants" $K^{\ddagger}_{OH}$ and $K^{\ddagger}_{B}$, which reflect pseudoequilibrium binding of an electrophilic catalyst M to the transition state of specific base or general base reaction with formation of transition states **1** or **2** (Scheme 2), are given by eqs 4 and 5, respectively, and logarithms of these constants are shown in Table 1.

$$K^{\ddagger}_{OH} = \frac{k_{M,OH}}{k_{OH}} \tag{4}$$

$$K^{\ddagger}_{B} = \frac{k_{M,B}}{k_{B}} \tag{5}$$

These "equilibrium constants" multiplied by the concentration of M give the real acceleration effect of the catalyst at this particular concentration and therefore serve as a direct measure of the efficiency of catalysis. One can notice that log $K^{\ddagger}_{OH}$ values, which refer to the formation of transition state **1** from a dianionic transition state of specific base reaction, are approximately twice as large as log $K^{\ddagger}_{B}$, which refer to the formation of transition state **2** from a monoanionic transition state of general base reaction. This is in agreement with mostly electrostatic stabilization by the electrophilic assistance. The absolute values of transition state binding constants for the specific base reaction are very large. To see how large may be the affinity of electrophilic species employed as catalysts toward a phosphate dianion, we measured the ground state association constants ($K_{NPP}$) of some of these species with 4-nitrophenyl phosphate (NPP) dianion giving complexes **3** (Scheme 2, R = 4-nitrophenyl). Dianions of phosphate monoesters $ROPO_3^{2-}$ are often considered as crude analogues of transition states of phosphodiester hydrolysis/transesterification reactions.[15] The respective values of log $K_{NPP}$ are collected in the last column of Table 1. First, one can notice that $K^{\ddagger}_{B}$ is smaller than $K_{NPP}$ both for M = $Mg^{2+}$ and M = guanidium cation in accordance with the larger negative charge (2−) of NPP compared to that of the general base transition state (1−), again in line with mostly electrostatic stabilization. Second, for the specific base reaction


dx.doi.org/10.1021/jo301649u | J. Org. Chem. 2012, 77, 9110−9119

**Table 2. Solvent Deuterium Kinetic Isotope Effects in Different Reaction Paths**

| 80% v/v DMSO | | | | | |
|---|---|---|---|---|---|
| | $k_{OH}/k_{OD}$ | $k_{M,OH}/k_{M,OD}$ | | $k_{M,B}^{H}/k_{M,B}^{D}$ | $k_{B}^{H}/k_{B}^{D}$ |
| M = | none | $Mg^{2+}$ | $Ca^{2+}$ | $Mg^{2+}$ | none |
| | 0.87 ± 0.02 | 0.25 ± 0.05 | 0.36 ± 0.05 | 1.23 ± 0.06 | 1.4[a] |
| water | | | | | |
| | $k_{OH}/k_{OD}$ | $k_{M,OH}/k_{M,OD}$ | | | |
| M = | none | $Mg^{2+}$ | $Ca^{2+}$ | $Co(NH_3)_6^{3+}$ | Guanidine $H^+$ |
| | 0.80 ± 0.04 | 0.42 ± 0.06 | 0.47 ± 0.05 | 0.65 ± 0.07 | 0.79 ± 0.07 |

[a]Reference 8.

with $Co(NH_3)_6^{3+}$ $K^{\ddagger}_{OH}$ is only 3 times larger than $K_{NPP}$, but with $Ca^{2+}$ and $Mg^{2+}$ $K^{\ddagger}_{OH}$ surpasses $K_{NPP}$ by more than 2 orders of magnitude. In other words, transition state affinity of $Co(NH_3)_6^{3+}$ corresponds mostly to simple ion-pairing, but $Ca^{2+}$ and $Mg^{2+}$ have much higher transition state affinity. A similar, although less pronounced, effect is observed in water (see below).

To get further insight into mechanisms of different reaction paths, solvent kinetic deuterium isotope effects (SKIE) on respective rate constants were measured, Table 2.

The SKIE for specific base reaction in the absence of metal ions ($k_{OH}/k_{OD}$) was determined by measurements in unbuffered solutions in the presence of 1−3 mM $OH^-$ or $OD^-$ in DMSO mixtures with $H_2O$ or $D_2O$, respectively. The observation of an inverse SKIE for this path agrees with reported for *cis*-4-hydroxytetrahydrofuran 3-phenyl phosphate $k_{OH}/k_{OD}$ = 0.51 in water at 50 °C[3] and $k_{OH}/k_{OD}$ = 0.54 for alkaline cleavage of HPNP at 25 °C.[16,17] This effect has several contributions. In accordance with mechanism in Scheme 1 (with [M] = 0) the expression for $k_{OH}$ is given by eq 6, and the expression for the isotope effect takes the form of eq 7.

$$k_{OH} = \frac{k_0 K_a^{SH}}{K_w} \tag{6}$$

$$\frac{k_{OH}}{k_{OD}} = \left(\frac{k_0^{H}}{k_0^{D}}\right)\left(\frac{K_a^{SH}}{K_a^{SD}}\right)\left(\frac{K_w^{D}}{K_w^{H}}\right) \tag{7}$$

The isotope effects in the acid dissociation constant of the substrate (hydroxyl group of HPNP) and in the autoprotolysis constant of water ($K_w$) likely compensate for each other, and the observed isotope effect should be close to $k_0^{H}/k_0^{D}$. The value $k_0^{H}/k_0^{D}$ = 0.95 was reported for transphosphorylation of 5′-UpG-3′ measured at pH 14 when the substrate hydroxyl is completely deprotonated.[18]

Isotope effects in the $Mg^{2+}$-catalyzed reaction were measured in piperidine/HCl buffer solution in order to separate effects in specific base and general base reactions. Values of $pK_a^{D}$ = 10.83 ± 0.03 for piperidinium cation and $pK_w^{D}$ = 20.25 ± 0.05 for autoprotolysis of water were obtained by potentiometric titrations of piperidinium chloride and DCl, respectively, in 80% v/v DMSO/$D_2O$ at 37 °C with 0.1 M $Me_4NCl$ supporting electrolyte. Previously reported respective values in 80% v/v DMSO/$H_2O$ are 9.88 and 18.77.[8] Thus, the isotope effects in the acid dissociation constants in the mixed solvent are approximately 0.5 logarithmic units larger than those typically observed in pure water.[19] With these values one can calculate the concentration of free $OD^-$ in the buffer at a given fraction of free base.

The results for $Mg^{2+}$ in piperidine buffer solution containing 40% free base in 80% v/v DMSO/$D_2O$ are shown in Figure 3 (solid squares). The slope of this line is smaller than that in $H_2O$ at the same fraction of free base indicating a normal although small SKIE in the general base reaction, but the intercept is larger pointing to an inverse isotope effect in specific base reaction. In fact, the concentration of free $OD^-$ is 2.8 times smaller in the mixture with $D_2O$ than the concentration of free $OH^-$ in the mixture with $H_2O$ at the same fraction of free base because of a larger isotope effect in $pK_w$ than in $pK_a$ of piperidinium, and the real isotope effect in $k_{M,OH}$ is significantly larger than it seems from the raw results in the Figure 3. The calculated isotope effects for both reactions are given in Table 2. The isotope effect for $Ca^{2+}$-catalyzed reaction was determined in a similar way and also is shown in Table 2.

The SKIE in general base reaction assisted by $Mg^{2+}$ is somewhat smaller than that for unassisted reaction with piperidine base (Table 2). Rather small by itself, SKIE for unassisted reaction is consistent with an early transition state expected for a reaction with strongly activated leaving group, and a smaller value in the presence of $Mg^{2+}$ points to an even earlier transition state for the catalytic reaction in agreement with decreased Brønsted slope for the latter (see below). Opposite SKIEs for $k_{M,OH}$ and $k_{M,B}$ rate constants confirm the correct assignments of the reaction paths based on formal kinetic study in the buffered systems. Isotope effects in specific base reaction are discussed later together with results in water.

Relatively high catalytic activity of $Mg^{2+}$ in the general base reaction allowed us to determine $k_{M,B}$ with this cation for different bases. Figure 4 shows the dependences of $k_{obs}$ for HPNP transesterification in the presence of 6 mM $Mg^{2+}$ on free base concentration obtained from experiments with variable total concentration of different buffers: 3-methoxypropylamine (3-MeOPA), 2-methoxyethylamine (2-MeOEA), morpholine, *p*-dimethylaminopyridine (DAP), and imidazole. All buffers except imidazole were employed at constant 30−70% fraction of the free base. Imidazole, which has very low basicity in this medium (see Table 2), was added as a free base to 0.1 M 3-methoxopropylamine buffer containing 30% free base (pH 10.0). The $pK_a$ values for all buffers determined by potentiometric titrations of their hydrochlorides in 80% v/v DMSO at 37 °C are given in Table 3 together with respective $k_{M,B}$ values.

Figure 5 shows the results for $k_{M,B}$ (solid squares), which fit to eq 8. For comparison also are shown previously reported plots for guanidinium-assisted reaction (open squares, slope = 0.69) and unassisted general base reaction (solid circles, slope = 0.77).


dx.doi.org/10.1021/jo301649u | J. Org. Chem. 2012, 77, 9110−9119

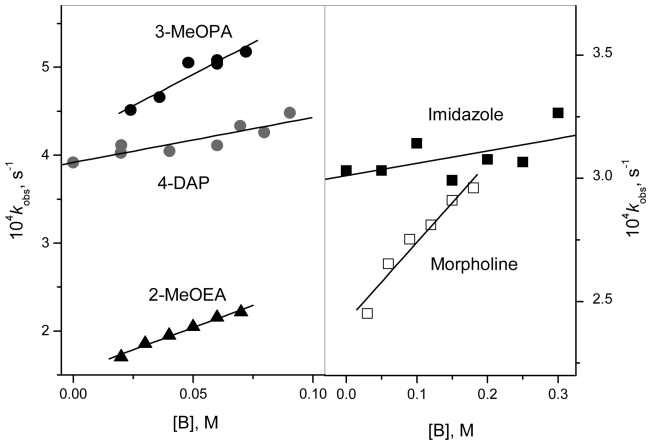


**Figure 4.** Observed rate constants in the presence of 6 mM $Mg^{2+}$ versus concentrations of different bases. [B] = [free base].

**Table 3. p$K_a$ Values of Protonated Forms of Different Bases and the Third-Order Rate Constants for HPNP Transesterification in the Presence of $Mg^{2+}$ in 80% v/v DMSO**

| | p$K_a$ | $k_{M,B}$ ($M^{-2}$ $s^{-1}$) |
|---|---|---|
| piperidine | 9.88 | 0.46 ± 0.05 |
| 3-MeOPA | 9.65 | 0.36 ± 0.03 |
| 2-MeOEA | 9.1 | 0.15 ± 0.02 |
| morpholine | 8.03 | 0.053 ± 0.003 |
| DAP | 7.46 ± 0.03 | 0.064 ± 0.013 |
| imidazole | 5.4 | 0.008 ± 0.004 |

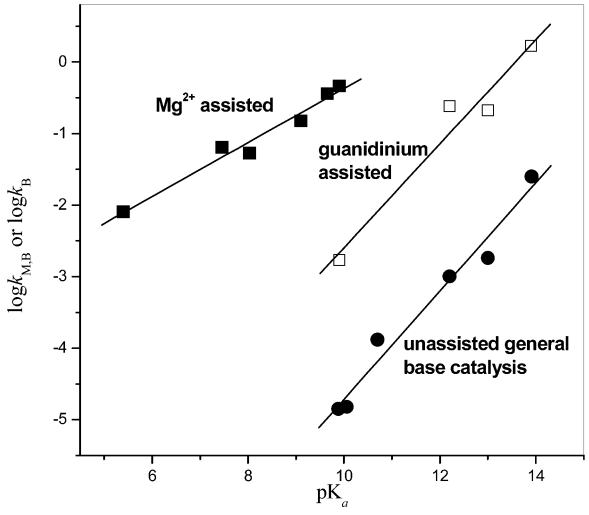


**Figure 5.** Brønsted plots for $Mg^{2+}$-assisted general base-catalyzed transesterification of HPNP in 80% DMSO. Data for guanidinium-assisted and unassisted reactions are from ref 8.

$$\log k_{M,B} = -4.1 \pm 0.3 + (0.38 \pm 0.03)pK_a \quad (8)$$

The slope of the Brønsted plots progressively decreases on going from unassisted general base reaction to guanidinium- and magnesium(II)-assisted reactions in accordance with expected shift to earlier transition state for stronger electrophilically activated reactions. An important consequence of this trend is that even weak bases such as imidazole and probably even nucleobases may participate in catalysis assisted by $Mg^{2+}$ in neutral solutions with reactivity typical for much stronger bases, which in neutral solutions are mostly protonated.

**Catalysis in Water.** The catalytic activity of alkaline earth cations in water is very low and can be conveniently measured at high free hydroxide concentrations. For this reason the catalytic rate constants for $Ca^{2+}$, $Co(en)_3^{3+}$, and $Co(NH_3)_6^{3+}$ were determined in unbuffered solutions at variable concentration of $Me_4NOH$ in the range 1−10 mM. Since $Mg^{2+}$ precipitates at pH above 10, its reactivity was measured in 0.1 M Tris buffer at pH 9−9.5. The reactivity of guanidinium chloride was measured in 0.1 M piperidine buffer in a pH range of 10.5−11.5 to avoid uncertainty in free hydroxide concentration, which may be reduced by partial deprotonation of guanidinium cation in highly basic solutions. The general base catalysis in HPNP transesterification in water is undetectable in 0.1 M and less concentrated buffer solutions in the background of much faster specific base reaction. In all cases we observed a simple first-order in catalyst and first-order in hydroxide kinetics (Figure 5S in Supporting Information) with third-order catalytic rate constants $k_{M,OH}$ shown in Table 4. Solvent deuterium isotope effects shown in Table 2 were determined for these rate constants under similar conditions.

**Table 4. Third-Order Rate Constants for HPNP Transesterificaiton in Water and Stability Constants of 4-Nitrophenyl Phosphate Complexes ($K_{NPP}$)**

| catalyst | $k_{M,OH}$ ($M^{-2}$ $s^{-1}$) | log $K^{\ddagger}_{OH}$ | log $K_{NPP}$ |
|---|---|---|---|
| $HGu^+$ | 0.37 ± 0.03 | 0.36 | 0.54[a] |
| $Co(NH_3)_6^{3+}$ | 26.7 ± 0.5 | 2.31 | 1.97 ± 0.04 |
| $Co(En)_3^{3+}$ | 61.7 ± 0.6 | 2.68 | 2.09 ± 0.06 |
| $Ca^{2+}$ | 85.2 ± 2.4 | 2.82 | 1.51 ± 0.03 |
| $Mg^{2+}$ | 153 ± 7 | 3.07 | 1.53 ± 0.03 |
| $Zn^{2+}$[b] | $6.7 \times 10^3$ | 4.71 | 1.76[c] |

[a]Reference 8. [b]Reference 20, at 25 °C. [c]Reference 21, at 25 °C.

There is an uncertainty in the case of guanidinium because the cation-assisted specific base mechanism is kinetically indistinguishable with general base catalysis by the neutral guanidine molecule. The interrelation between the rate constants is given by the eq 9 where B and BH are neutral and protonated guanidine and $K_a^{BH}$ is the acid dissociation constant of guanidinium cation.

$$k_B = k_{BH,OH}\left(\frac{K_w}{K_a^{BH}}\right) \quad (9)$$

With p$K_a$ 13.3 at 37 °C for guanidinium cation[22] one obtains $k_B$ = 0.19 $M^{-1}$ $s^{-1}$ in water, which is not far from $k_B$ = 0.025 $M^{-1}$ $s^{-1}$ for guanidine free base in 80% v/v DMSO reported in ref 8. However, the latter rate constant has the normal solvent isotope effect of 1.7,[8] while the reaction in water has the inverse isotope effect (Table 2) typical for specific base reaction.

The inverse SKIE measured for $k_{OH}$ is smaller than the reported value 0.54 at 25 °C for the same HPNP substrate.[16,17] Repeating measurements at 25 °C we found a closer value of 0.74, which however is still significantly different from the reported one. A probable reason is different methodology of measurement. The value reported in ref 16 was determined from rate constants measured in $H_2O$ and $D_2O$ at pH = pD with pD calculated by the usually applied correction factor 0.4, while we calculated the isotope effect as the ratio of second-order rate constants measured by varying total [$OH^-$] or total


dx.doi.org/10.1021/jo301649u | J. Org. Chem. 2012, 77, 9110−9119

[$OD^-$] taken at high excess over [HPNP] in respective solvents. There are concerns that the correction term for pD actually depends on temperature and glass properties of the electrode and is not a universal constant.[3,23] Measurements with known total concentration of hydroxide are free from this possible error. In any case, it is clear that the general base reaction has a significant inverse SKIE.

Other relevant reported data involve SKIE 1.43 for HPNP cleavage in the presence of a Zn(II) complex at high pH when the complex is totally converted into the hydroxo form[16] and SKIE reported for transesterification of the chemically similar to HPNP substrate uridine 3′,4-nitrophenyl phosphate (UpPNP) catalyzed by a Zn(II) binuclear complex at variable pH.[4] For the latter system SKIE is 0.8 at high pH when the complex is mostly in hydroxo form and 3.2 at pH = pD = 7.1 when the complex is mostly in the aquo form. Assuming that in both systems the reaction proceeds in accordance with the mechanism in Scheme 1 and the active form of the catalyst is the aquo complex, which undergoes deprotonation to inactive hydroxo complex (eq 10) with dissociation constant $K_{a,M}$, the expression for the observed second-order rate constant of the catalytic reaction takes the form of eq 11.

$$M^{n+} \rightleftarrows M(OH)^{n-1} + H^+ \tag{10}$$

$$k_2 = k_C\left(\frac{\frac{K_a^{SH}}{[H^+]}}{\frac{1+K_{a,M}}{[H^+]}}\right) \tag{11}$$

Under conditions of complete deprotonation of the catalyst at high pH eq 10 takes the form of eq 12, and the expression for SKIE is eq 13.

$$k_2 = k_C\left(\frac{K_a^{SH}}{K_{a,M}}\right) \tag{12}$$

$$\frac{k_2^H}{k_2^D} = \left(\frac{k_C^H}{k_C^D}\right)\left(\frac{K_a^{SH}}{K_a^{SD}}\right)\left(\frac{K_{a,M}^D}{K_{a,M}^H}\right) \tag{13}$$

In eq 13 equilibrium isotope effects in dissociation constants of the substrate and catalyst partially compensate for each other, but since the substrate is a much weaker acid its dissociation constant is expected to have a larger isotope effect[19] and therefore the actual SKIE in catalytic rate constants $k_C^H/k_C^D$ should be a smaller number than the observed SKIE. This means that for Zn(II)-catalyzed cleavage of UpPNP $k_C^H/k_C^D$ is smaller than 0.8, and for catalytic HPNP cleavage $k_C^H/k_C^D$ most probably is below unity.

Under conditions of negligible deprotonation of the catalyst at low pH eq 11 takes the form of eq 14:

$$k_2 = k_C\left(\frac{K_a^{SH}}{[H^+]}\right) = k_C\left(\frac{K_a^{SH}}{K_W}\right)[OH^-] = k_{M,OH}[OH^-] \tag{14}$$

It follows from eq 14 that

$$k_{M,OH} = \frac{k_2}{[OH^-]} = k_C\left(\frac{K_a^{SH}}{K_W}\right) \tag{15}$$

The SKIE calculated as the ratio $k_2^H/k_2^D$ at pH = pD equals $(k_C^H/k_C^D)(K_a^{SH}/K_a^{SD})$ and it is easy to see from the eq 15 that the respective SKIE in the third-order rate constant $k_{M,OH}$ can be calculated according to eq 16:

$$\frac{k_{M,OH}}{k_{M,OD}} = \left(\frac{k_2^H}{k_2^D}\right)_{pH=pD}\left(\frac{K_w^D}{K_w^H}\right) \tag{16}$$

With $K_w^D/K_w^H = 0.135$ at 25 °C[24] one obtains from $k_2^H/k_2^D = 3.2$ the value of $k_{M,OH}/k_{M,OD} = 0.43$ for Zn(II)-catalyzed cleavage of UpPNP, which is very close to SKIE determined for $Mg^{2+}$- and $Ca^{2+}$-catalyzed HPNP cleavage (Table 2).

Considering results shown in Table 2 for the specific base reaction both in aqueous DMSO and water together with the above cited literature data one concludes that the inverse SKIE in general becomes stronger in the presence of metal ions providing the Lewis acid assistance. Reactions in the presence of "protic" electrophilic catalysts $Co(NH_3)_6^{3+}$ and guanidinium cation have only a little bit larger inverse isotope effects than the unassisted reaction. The inverse solvent deuterium effect is normally observed in specific base reactions[25] and is attributed to the fact that hydroxide anion is a stronger base in $D_2O$ than in $H_2O$.[26] This should be valid also for the alkoxide anion. An increase in the isotope effect in the presence of metal ions may be related to additional inverse equillibrium isotope effect of metal ion association with the anionic transition state. To test this hypothesis we measured the association constants of $Mg^{2+}$ with NPP dianion in $H_2O$ and $D_2O$ under similar conditions (37 °C, ionic strength 0.1M) and obtained log $K_{NPP}^H = 1.53 \pm 0.01$ and log $K_{NPP}^D = 1.63 \pm 0.01$, which correspond to a modest inverse solvent isotope effect of 0.79 ± 0.03. Stronger inverse equilibrium isotope effects are observed, however, for hydroxide association with metal ions. Indeed, the deprotonation equilibrium (9) is equivalent to the equilibrium of association of the metal ion (or metal complex) with hydroxide anion with the equilibrium constant $K_{MOH} = K_{a,M}/K_w$. The equilibrium isotope effect in $K_{MOH}$ equals therefore that in $K_{a,M}$, typically about 3,[4] divided by the isotope effect 7.4 in $K_w$,[24] which gives the inverse isotope effect about 0.4. A similar effect may be expected for association between metal ions and alkoxide anions and therefore we consider the increased inverse SKIE in specific base reaction assisted by metal ions as an evidence of the contact between the metal ion and entering alkoxide nucleophile in the transition state. This hypothesis finds some support from the correlation analysis between $K^{\ddagger}_{OH}$ and $K_{NPP}$ values discussed below.

**Correlation between Transition State "Binding Constants" and Binding Constants of Catalysts to a Transition State Analogue.** Table 4 contains the stability constants of NPP complexes measured under similar conditions and includes also literature data for $Zn^{2+}$ for comparison. Inspection of the results in Table 4 shows that the catalytic activity of Co(III) complexes operating through the outer-sphere mechanism is 2 orders of magnitude larger than that of guanidinium cation, and accordingly these complexes have much higher affinity to the transition state model NPP than the guanidinium cation. However, Co(III) complexes also bind NPP tighter than $Ca^{2+}$, $Mg^{2+}$, and even $Zn^{2+}$ but have much lower catalytic activity. To see a more general picture we attempted to correlate log $K^{\ddagger}_{OH}$ versus log $K_{NPP}$ for all the reported so far catalytic systems for HPNP transesterification for which the respective data are available. Besides the results collected in Tables 1 and 4 these involve data for Zn(II) complexes shown in Chart 1. The phosphate monoesters employed as transitions state models for these complexes were $MeOPO_3^{2-}$ or $PhOPO_3^{2-}$ instead of NPP ($4\text{-}O_2NC_6H_4OPO_3^{2-}$); however, the binding constants of $Mg^{2+}$, $Ca^{2+}$, and $Zn^{2+}$ to


dx.doi.org/10.1021/jo301649u | J. Org. Chem. 2012, 77, 9110−9119

**Chart 1**

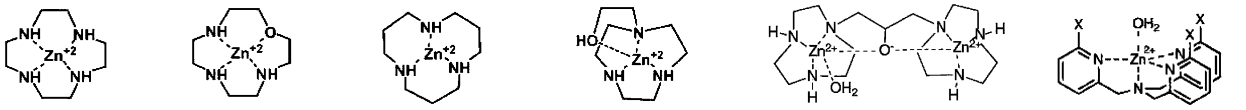

$ZnL^1$ $ZnL^2$ $ZnL^3$ $ZnL^4$ $Zn_2L$ ZnPy(X=H)

$ZnPyNH_2$ ($X=NH_2$)

these ligands vary within limits of a factor of 2.5 for a given metal ion,[21] which is insignificant in the scale of the observed catalytic effects.

Figure 6 shows the whole set of data. Red points correspond to results obtained in 80% v/v DMSO, and other results are for

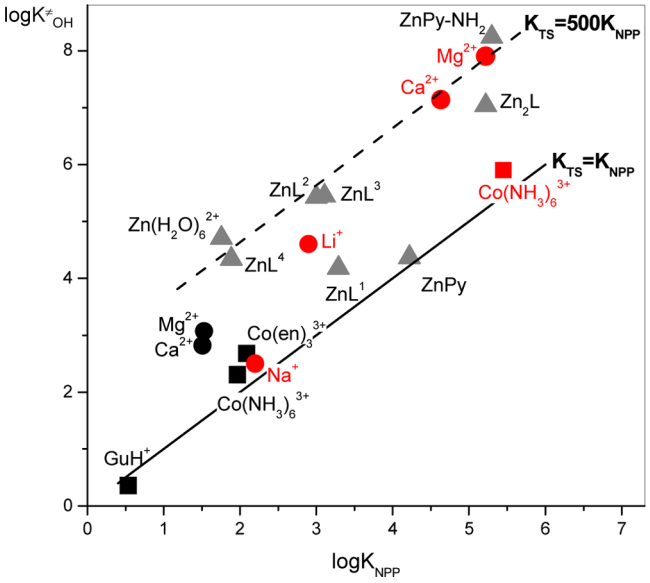


**Figure 6.** Correlation between binding constants of catalysts to the transition state ($K^{\ddagger}_{OH}$) and to a transition state model ($K_{NPA}$) for transesterification of HPNP via specific base mechanism. Red points correspond to results in 80% v/v DMSO. Data for Zn(II) complexes (Chart 1) are from refs 15 and 20.

aqueous solutions. The solid line corresponds to the situation when $\log K^{\ddagger}_{OH} = \log K_{NPP}$. The catalysts that fit to this line are all "protic" electrophiles (guanidinium, $Co(NH_3)_6^{3+}$, $Co(en)_3^{3+}$), $Na^+$, and Zn(II) complexes with tetradentate ligands ($ZnL^1$ and ZnPy). All these species bind the transition state of specific base reaction with the same affinity as the phosphate monoester, which can be interpreted in terms of close similarity between the binding modes in complexes **1** and **3**. These species seem to be unable to use for transition state binding more donor atoms than equatorial phosphorane oxygens. The correlation spans over 5 orders of magnitude in $K^{\ddagger}_{OH}$ and $K_{NPP}$ and includes results both for water and aqueous DMSO.

On the other hand, Zn(II) complexes with tridentate ligands ($ZnL^2$, $ZnL^3$, $ZnL^4$), free $Zn^{2+}$ aquocation, and Zn(II) complexes "enforced" by binuclearity ($Zn_2L$) or by incorporation of additional proton donor groups in *ortho* positions of pyridine ligands ($ZnPyNH_2$) clearly form another correlation line shown by a dashed line shifted upward by 2.7 logarithmic units. In other words, catalysts of this series bind the transition state 500 times stronger than the monoester analogue. Interestingly, $Ca^{2+}$ and $Mg^{2+}$ in aqueous DMSO fall on this line, while $Li^+$ in DMSO and $Ca^{2+}$ and $Mg^{2+}$ in water occupy intermediate positions. The unity slopes of both lines mean that within each family of catalysts the improvements provided by ligand or medium effects to the catalytic activity (transition state binding) are of the same type, which is required for better binding of dianion of phosphate monoester, but there is an intrinsic difference in the type of binding between these two groups, which makes possible the approximately 3 orders of magnitude stronger transition state binding for the catalysts of the second group. The most evident structural difference between the transition state and its model is that in the former the negative charge is distributed not only over phosphoryl oxygens, but to a large extent is localized also on the entering alkoxide oxygen. It is possible therefore that the advantage of $Zn^{2+}$, coordinative unsaturated Zn(II) complexes, $Mg^{2+}$ and $Ca^{2+}$ cations is their ability to polydentate coordination, which allows them to make use of an additional donor atom as illustrated schematically in structure **4**. This hypothesis agrees with increased inverse SKIE of $Mg^{2+}$- and $Ca^{2+}$-assisted specific base reactions (see above).

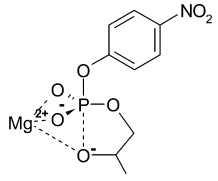

**4**

An additional observation worth mentioning is that the transition state stabilization by $Mg^{2+}$ in aqueous DMSO is similar to that of most active Zn(II) complexes in water, indicating the importance of solvation effects for electrophilic assistance to nucleophilic substitution at the phosphoryl group. Finally, the utility of using phosphate monoesters as transition state analogues is manifested also in the observation of a good correlation between catalytic activity and affinity of metal ions to a phosphate monoester for RzB HH ribozyme cleavage.[1a]

## CONCLUSION

The major point of this study is the demonstration of the unique ability of $Mg^{2+}$ to assist the general base-catalyzed transesterification of a phosphodiester. Such a mechanism is considered for, e.g., colicin E7 and I-Pol nucleases,[1f] as well as for self-cleaving ribozymes.[27] The most important aspect of this assistance effect is the low slope of the Brønsted plot, which makes possible an efficient catalysis by weakly basic catalysts. This may have implications for ribozyme catalysis, explaining why such poor bases as the nucleobases can be catalytically active. The correlation analysis based on comparison of transition state "binding constants" and ground state binding


dx.doi.org/10.1021/jo301649u | J. Org. Chem. 2012, 77, 9110–9119

constants of catalysts to a transition state analogue previously employed for some particular catalysts proved to be a useful tool for identification of the nature of catalyst−transition state interaction with catalysts of different types and may find further applications in mechanistic analysis of chemical and biological phosphate ester cleaving systems.

Solvent kinetic isotope effects serve well to confirm the assignment of general base and specific base reaction paths in the presence of metal ions inferred from formal kinetic studies. A small decrease by ca. 15% in SKIE for the general base reaction in the presence of $Mg^{2+}$ most probably reflects an earlier transition state of the catalytic reactions, in agreement with a decreased Brønsted slope. A significant increase in the inversed SKIE for Lewis acid assisted specific base reaction can be a general phenomenon in phosphodiester transestericiation, but the origin of this effect is not entirely clear. At least partly it can be attributed to inverse equilibrium solvent isotope effect in metal ion−anionic transition state association by analogy with inverse isotope effects observed for metal ion association with phosphate monoester and hydroxide anions, but the reason for the latter is uncertain. The major contribution to inverse SKIE in specific base reactions comes from the anionic nucleophile solvation.[25] Probably similar solvation effects of the anionic transition state are responsible for the above mentioned equilibrium effect.

## EXPERIMENTAL SECTION

**General Experimental Methods.** 2-Hydroxypropyl 4-nitophenyl phosphate (HPNP) was prepared as the barium salt according to the literature procedure.[28] Guanidinium chloride, piperidine hydrochloride, other amines employed as buffers, metal salts, $Me_4N(OH)\cdot 5H_2O$, $Me_4NCl$, $D_2O$ (99.9% D), and $p$-$O_2NC_6H_4OPO_3Na_2$ were used as supplied. DMSO (Baker) was purified by distillation over CaO followed by 72 h sequential drying over 4 Å molecular sieves.[29]

**Potentiometry.** Potentiometric titrations were performed in a 30-mL thermostatted cell kept under nitrogen at 37 ± 0.1 °C with 0.01 M $Me_4NCl$ as background electrolyte. Experimental details and procedure for the electrode calibration were the same as in refs 30 and 31. The program Hyperquad 2003[32] was used to calculate all equilibrium constants. Determinations of association constants of $p$-$O_2NC_6H_4OPO_3^{2-}$ with all cations in water and with $Co(NH_3)_6^{3+}$ in aqueous DMSO were performed by titrations of 1−10 mM $p$-$O_2NC_6H_4OPO_3H_2$ (obtained by passing the sodium salt through a column with Amberlite IR-120H ion-exchange resin) alone and in the presence of 1−10 mM of metal salts. Determination of association constants with $Mg^{2+}$ and $Ca^{2+}$ in 80% v/v DMSO by this technique was impossible because of precipitation of $p$-$O_2NC_6H_4OPO_3M$ salts and these constants were determined by spectrophotometric titrations at lower concentrations in buffered solutions at sufficiently low pH (see below).

**Kinetics.** Kinetic measurements were performed on a Hewlett-Packard 8453 diode array spectrophotometer equipped with a thermostatted cell compartment at 37.0 ± 0.1 °C. Reaction solutions were prepared by combining appropriate amounts of the metal salt, background electrolyte ($Me_4NCl$) and buffer or tetramethylammonium hydroxide stock solutions to the desired volume in water or 80% v/v DMSO at constant ionic strength 0.1 M. Reactions were initiated by adding an aliquot of the substrate solution. Stock solutions of HPNP were freshly prepared in water and passed through Amberlite IR-120H ion-exchange resin to remove $Ba^{2+}$ cation, which causes interference in aqueous DMSO.[33] The exact concentration of HPNP was determined from absorbance of $p$-nitrophenolate anion after complete hydrolysis by 0.1 M NaOH of an aliquot taken from the stock solution. The course of transesterification of HPNP was monitored spectrophotometrically by the appearance of 4-nitrophenolate anion at 404 nm (in water) or 420 nm (in 80% DMSO). The HPNP prepared as described by Brown[28] contains ca. 5% of 1-hydroxy-2-propyl isomer, which is ca. 10 times more reactive than the main 2-hydroxypropyl isomer.[34] The presence of this minor isomer affects significantly the initial reaction rate used for studies of slow kinetics. For this reason we used for measurements of the initial rates the stock solutions of HPNP prehydrolyzed by ca. 30% to reduce the content of the rapidly reacting isomer to a negligible amount. The integral kinetics were fitted to the eq 17 where $\Delta A$ is the observed change in the absorbance at time $t$, $\Delta A_1$ and $\Delta A_2$ are the absorbance changes due to complete hydrolysis of minor and major isomers, respectively, $k_{fast}$ and $k_{slow}$ are the first-order rate constants of hydrolysis of these isomers, and $t$ is the reaction time. The value of $k_{slow}$ for the major slower reacting isomer was considered as the observed first-order rate constants ($k_{obs}$) for the transesterification of HPNP.

$$\Delta A = \Delta A_1(1 - e^{-k_{fast}t}) + \Delta A_2(1 + e^{-k_{slow}t}) \quad (17)$$

**Spectrophotometric Titrations.** Determinations of association constants of $Mg^{2+}$ and $Ca^{2+}$ with $p$-$O_2NC_6H_4OPO_3^{2-}$ is 80% v/v DMSO were performed by spectrophotometric titrations of 0.1 mM $p$-$O_2NC_6H_4OPO_3H_2$ in morpholine buffer at pH 8.0 and 37 °C by metal salts. The observed association constants were corrected for the degree of protonation of the phosphate monoester with known $pK_a$ = 10.6 [8] of $p$-$O_2NC_6H_4OPO_3H_2$ under these conditions.

## ASSOCIATED CONTENT

### Supporting Information

Rate constants for $Li^+$-, $Na^+$-, and $Co(en)_3^{3+}$-assisted reactions in 80% v/v DMSO as function of free base fraction; rate constants for all catalysts studied in water as function of free hydroxide concentration. This material is available free of charge via the Internet at http://pubs.acs.org.

## AUTHOR INFORMATION

### Corresponding Author

*E-mail: anatoli@unam.mx.

### Notes

The authors declare no competing financial interest.

## ACKNOWLEDGMENTS

Financial support by DGAPA-UNAM (project IN 203408) is gratefully acknowledged.

## REFERENCES

(1) (a) Schnabl, J.; O Sigel, R. K. O. *Curr. Opin. Chem. Biol.* **2010**, *14*, 269−275. (b) Sigel, R. K. O.; Pyle, A. M. *Chem. Rev.* **2007**, *107*, 97−113. (c) Oivanen, M.; Kuusela, S.; Lönnberg, H. *Chem. Rev.* **1998**, *98*, 961−990. (d) Cowan, J. A. *BioMetals* **2002**, *15*, 225−235. (e) Cowan, J. A. *Chem. Rev.* **1998**, *98*, 1067−1087. (f) Dupureur, C. M. *Curr. Opin. Chem. Biol.* **2008**, *12*, 250−255.

(2) Bruice, T. C.; Benkovic, S. J. *Bioorganic Mechanisms*; W. A. Benjamin, Inc.: New York, 1966; Vol. 2, pp 37−48.

(3) Usher, D. A.; Richardson, D. I., Jr.; Oakenfull, D. G. *J. Am. Chem. Soc.* **1970**, *92*, 4699−4712.

(4) Yang, M. −Y.; Iranzo, O.; Richard, J. P.; Morrow, J. R. *J. Am. Chem. Soc.* **2005**, *127*, 1064−1065.

(5) (a) Perreault, D. M.; Anslyn, E. V. *Angew. Chem., Int. Ed. Engl.* **1997**, *36*, 432−450. (b) Kosonen, M.; Yousefi-Salakdeh, E.; Strömberg, R.; Lönnberg, H. *J. Chem. Soc., Perkin Trans. 2* **1998**, 1598−1595.

(6) (a) Kirby, A. J.; Marriott, R. E. *J. Chem. Soc., Perkin Trans. 2* **2002**, 422−427. (b) Beckmann, C.; Kirby, A. J.; Kuusela, S.; Tickle, D. C. *J. Chem. Soc., Perkin Trans. 2* **1998**, 573−581.

(7) Kuusela, S.; Rantanen, M.; Lönnberg, H. *J. Chem. Soc. Perkin Trans. 2* **1995**, 2269−2273.

(8) Corona-Martínez, D. O.; Taran, O.; Yatsimirsky, A. K. *Org. Biomol. Chem.* **2010**, *8*, 873−880.

(9) Jou, R.; Cowan, J. A. *J. Am. Chem. Soc.* **1991**, *123*, 6685−6686.
(10) Saito, H.; Suga, H. *Nucleic Acids Res.* **2002**, *30*, 5151−5159.
(11) Gomez-Tagle, P.; Vargas-Zúñiga, I.; Taran, O.; Yatsimirsky, A. K. *J. Org. Chem.* **2006**, *71*, 9713−9722.
(12) (a) Ariga, K.; Anslyn, E. V. *J. Org. Chem.* **1992**, *57*, 417−419. (b) M. Kneeland, D. M.; Ariga, K.; Lynch, V. M.; Huang, C.−Y.; Anslyn, E. V. *J. Am. Chem. Soc.* **1993**, *115*, 10042−10055.
(13) (a) Wolfenden, R. *Acc. Chem. Res.* **1972**, *5*, 10−18. (b) Lienhard, G. E. *Science* **1973**, *180*, 149−154. (c) Mader, M. M.; Bartlett, P. A. *Chem. Rev.* **1997**, *97*, 1281−1302.
(14) (a) Kurz, J. L. *Acc. Chem. Res.* **1972**, *5*, 1−9. (b) Yatsimirsky, A. K. *Coord. Chem. Rev.* **2005**, *249*, 1997−2011.
(15) (a) Yang, M. −Y.; Morrow, J. R.; Richard, J. P. *Bioorg. Chem.* **2007**, *35*, 366−374. (b) Feng, G.; Mareque−Rivas, J. C.; Torres Martín de Rosales, R.; Williams, N. H. *J. Am. Chem. Soc.* **2005**, *127*, 13470−13471.
(16) Bonfa, L.; Gatos, F.; Mancin, F.; Tecilla, P.; Tonellato, U. *Inorg. Chem.* **2003**, *42*, 3943−3949.
(17) Calculated from $k_{obs}^{H}/k_{obs}^{D}$ = 4 measured at pH = pD = 9.0 reported in ref 16 by using the equation $k_{OH}/k_{OD} = (k_{obs}^{H}/k_{obs}^{D})(K_w^{D}/K_w^{H})$ with $K_w^{D}/K_w^{H}$ = 0.135 at 25 °C according to ref 24.
(18) Harris, M. E.; Dai, Q.; Gu, H.; Kellerman, D. L.; Piccirilli, J. A.; Anderson, V. E. *J. Am. Chem. Soc.* **2010**, *132*, 11613−11621.
(19) Jencks, W. P. *Catalysis in Chemistry and Enzymology*, Dover: New York, 1987; p 250.
(20) Mathews, R. A.; Rossiter, C. S.; Morrow, J. R.; Richard, J. P. *Dalton Trans.* **2007**, 3804−3811.
(21) Massoud, S. S.; Sigel, H. *Inorg. Chem.* **1988**, *27*, 1447−1453.
(22) (a) Davis, T. L.; Elderfield, R. C. *J. Am. Chem. Soc.* **1932**, *54*, 1499−1503. (b) Albert, A.; Goldacre, R.; Phillips, J. *J. Chem. Soc.* **1948**, 2240−2249.
(23) Baucke, F. G. K. *J. Phys. Chem. B* **1998**, *102*, 4835−4841.
(24) Covington, A. K.; Robinson, R. A.; Bates, R. G. *J. Phys. Chem.* **1966**, *70*, 3820−3824.
(25) Slebocka-Tilk, H.; Neverov, A. A.; Brown, R. S. *J. Am. Chem. Soc.* **2003**, *125*, 1851−1858.
(26) Swin, C. G.; Bader, R. F. W. *Tetrahedron* **1960**, *10*, 182−199.
(27) Chval, Z.; Chvalova, D.; Leclerc, F. *J. Phys. Chem. B* **2011**, *115*, 10943−10956.
(28) Brown, D. M.; Usher, D. A. *J. Chem. Soc.* **1965**, 6558−6564.
(29) Burfield, D. R.; Smithers, R. H. *J. Org. Chem.* **1978**, *43*, 3966−3968.
(30) Sánchez-Lombardo, I.; Yatsimirsky, A. K. *Inorg. Chem.* **2008**, *47*, 2514−2525.
(31) Gomez-Tagle, P.; Yatsimirsky, A. K. *Inorg. Chem.* **2001**, *40*, 3786−3796.
(32) Gans, P.; Sabatini, A.; Vacca, A. *Talanta* **1996**, *43*, 1739−1753.
(33) Taran, O.; Medrano, F.; Yatsimirsky, A. K. *Dalton Trans.* **2008**, 6609−6618.
(34) Williams, N. H. Personal communication.